

Cr₂O₃ 和 CrO₃/Cr₂O₃ 催化剂的 2-氯-1,1,1-三氟乙烷气相氟化反应的活性物种和失活

汪 云¹ 梁 艳¹ 何 军² 张文霞¹ 罗建伟¹ 鲁继青¹ 罗孟飞^{*,1}

(¹ 浙江师范大学物理化学研究所, 教育部先进催化材料重点实验室, 金华 321004)

(² 台州出入境检验检疫局, 台州 318000)

摘要: 采用沉淀法和浸渍法制备了 2 种铬基(Cr₂O₃ 和 CrO₃/Cr₂O₃)催化剂, 用于气相氟化 2-氯-1,1,1-三氟乙烷合成 1,1,1,2-四氟乙烷。研究发现含有低价铬(Cr³⁺)物种的 Cr₂O₃ 催化剂上 2-氯-1,1,1-三氟乙烷的稳态转化率为 18.5%, 而含有高价铬(Cr⁶⁺)物种和低价铬(Cr³⁺)物种的 CrO₃/Cr₂O₃ 催化剂初始转化率达到 30.6%, 然而存在明显的失活。含有 Cr⁶⁺物种的 CrO₃/Cr₂O₃ 催化剂的 2-氯-1,1,1-三氟乙烷氟化反应初始 TOF 值为 $1.71 \times 10^{-4} \text{ mol}_{\text{HCFC-133a}} \cdot \text{mol}_{\text{Cr(VI)}}^{-1} \cdot \text{s}^{-1}$, 高于含有 Cr³⁺物种的 Cr₂O₃ 催化剂($4.16 \times 10^{-5} \text{ mol}_{\text{HCFC-133a}} \cdot \text{mol}_{\text{Cr(III)}}^{-1} \cdot \text{s}^{-1}$)。Cr₂O₃ 催化剂在氟化反应前后催化剂的物相结构保持不变; 而含有高价铬物种的 CrO₃/Cr₂O₃ 催化剂经 HF 反应后生成了 CrO_xF_y 活性物种。然而, CrO_xF_y 物种在反应中挥发或转化成稳定但无活性的 CrF₃, 从而导致催化剂失活。

关键词: Cr₂O₃; CrO₃/Cr₂O₃; 氟化; HCFC-133a; HFC-134a; 催化剂失活

中图分类号: O643.32 **文献标识码:** A **文章编号:** 1001-4861(2017)01-0123-11

DOI: 10.11862/CJIC.2016.281

Catalytic Behaviors of Cr₂O₃ and CrO₃/Cr₂O₃ Catalysts for Gas Phase Fluorination of 2-Chloro-1,1,1-trifluoroethane: Active Species and Catalyst Deactivation

WANG Yun¹ LIANG Yan¹ HE Jun² ZHANG Wen-Xia¹

LUO Jian-Wei¹ LU Ji-Qing¹ LUO Meng-Fei^{*,1}

(¹Key Laboratory of the Ministry of Education for Advanced Catalysis Materials, Institute of Physical Chemistry, Zhejiang Normal University, Jinhua, Zhejiang 321004, China)

(²Taizhou Entry-Exit Inspection and Quarantine Bureau, Taizhou, Zhejiang 318000, China)

Abstract: Two Cr-based model catalysts (Cr₂O₃ and CrO₃/Cr₂O₃) were prepared respectively by precipitation and impregnation method and tested for gas phase fluorination of 2-chloro-1,1,1-trifluoroethane to synthesize 1,1,1,2-tetrafluoroethane. It was found that the Cr₂O₃ catalyst containing low valent Cr species (Cr³⁺) was stable during the reaction with a steady state conversion of 18.5%. On the contrary, the CrO₃/Cr₂O₃ catalyst containing both high valent Cr species (Cr⁶⁺) and low valent Cr species (Cr³⁺) had higher initial activity (30.6%) but it deactivated rapidly, with the same activity as the Cr₂O₃ catalyst at steady state. Moreover, quantitative analyses showed that the Cr⁶⁺ species in the CrO₃/Cr₂O₃ catalyst had an initial turnover frequency of $1.71 \times 10^{-4} \text{ mol}_{\text{HCFC-133a}} \cdot \text{mol}_{\text{Cr(VI)}}^{-1} \cdot \text{s}^{-1}$, which was much higher than that of the Cr³⁺ species ($4.16 \times 10^{-5} \text{ mol}_{\text{HCFC-133a}} \cdot \text{mol}_{\text{Cr(III)}}^{-1} \cdot \text{s}^{-1}$) in the Cr₂O₃ catalyst. In addition, the characterization results revealed that the Cr₂O₃ remained its structure while the high valent Cr species in the CrO₃/Cr₂O₃ reacted with HF to form catalytically active CrO_xF_y species. However, such CrO_xF_y

收稿日期: 2016-06-23。收修改稿日期: 2016-10-28。

国家自然科学基金(No.21373186)资助项目。

*通信联系人。E-mail: mengfeiluo@zjnu.cn

species could either volatilize during the reaction or transformed to stable but inactive CrF_3 , which accounted for the catalyst deactivation.

Keywords: Cr_2O_3 ; $\text{CrO}_3/\text{Cr}_2\text{O}_3$; fluorination; HCFC-133a; HFC-134a; catalyst deactivation

0 Introduction

The catalytic gas phase F/Cl exchange reaction is very important in the synthesis of new generation refrigerants^[1-6], in which Cr-based catalysts are commonly employed^[7-10]. For chromium oxides, Cr species mainly exist in forms of Cr(VI) and Cr(III), such as CrO_3 and Cr_2O_3 ^[11]. The Cr-based catalysts for the vapor phase synthesis of hydrofluorocarbons mainly include unsupported chromium oxides and those supported on various materials^[12-16]. Moreover, it has been recognized that oxidation states of the Cr species have great influences on the catalytic behaviors in F/Cl exchange reactions. For example, high valent Cr species (*e.g.* Cr(VI)) have high reactivity^[17-19], while low valent Cr species (*e.g.* Cr(III)) are believed to be inactive^[20], but they are active for selective hydrogenation and methanol synthesis^[21-22]. Quan et al.^[17] compared the properties of chromium oxides treated in different atmospheres and they found that Cr(VI) species showed higher catalytic activities for the F/Cl exchange reaction than Cr(III). The role of high valent Cr species in the reaction was also investigated in our previous study^[23]. It was found that highly dispersed Cr(VI) species in the $\text{CrO}_x\text{Y}_2\text{O}_3$ catalyst transformed to Cr(V) and Cr(III) species under high temperature calcination, which resulted in a dramatic decline in the reactivity for the fluorination of 2-chloro-1,1,1-trifluoroethane. The importance of such high valent Cr species lies the fact that they could be further transformed to CrO_xF_y compounds via the reaction with HF, which are believed to be active species for F/Cl exchange reactions^[24-26]. However, such CrO_xF_y compounds are unstable under working conditions. Albonetti et al.^[27] reported that highly dispersed CrO_3 could easily react with HF to form CrO_2F_2 that is gaseous at room temperature, which is the main reason for the loss of Cr species during the reaction and consequently the catalyst deactivation.

The nature of the active species and their possible transformation during the reaction remain unclear. Firstly, CrO_xF_y compounds originated from Cr(VI) are generally recognized as the active species while Cr_2O_3 are inactive^[23]; while other researches pointed out that low valent Cr species such as Cr_2O_3 also have high reactivity. For example, our previous work revealed that crystalline Cr_2O_3 obtained at high calcination temperature also showed high F/Cl exchange reaction activity^[28]. Therefore, the identification of the contributions of Cr species is desirable to obtain a better understanding of the different roles in the reaction, which will be ideal if a quantitative analysis could be conducted. Secondly, in addition to the loss of volatile CrO_xF_y compounds, the transformation mechanism of CrO_xF_y under working conditions and the resulting compounds need further clarification.

To illustrate the different roles of Cr species in the F/Cl exchange reaction, delicately designed catalysts are necessary. The currently employed Cr catalysts are usually obtained by precipitating Cr precursors such as $\text{Cr}(\text{NO}_3)_3$ with further calcination. The resulting samples often contain a mixture of CrO_x oxides with different oxidation states, which leads to complexity in the investigation. In this work, we prepared two catalysts with distinct Cr_2O_3 and CrO_3 compositions which represent low and high valent Cr species. The comparison of the catalytic behaviors of these two catalysts provided useful information on the roles of different Cr species in the F/Cl exchange reaction. Moreover, the catalyst stability was investigated and the transformation of Cr species during the reaction was also discussed.

1 Experimental

1.1 Catalyst preparation

The Cr_2O_3 support was prepared by a precipitation method. A detailed process was as follows: $\text{Cr}(\text{NO}_3)_3 \cdot$

$9\text{H}_2\text{O}$ (analytical grade, Sinopharm Chemical Reagent Co., Ltd., China) was added to a 10% ammonia aqueous solution (Lanxi Yongli Chemical Co., LTD., China) under stirring until a precipitated slurry was obtained. The resulting slurry was aged for 2 h at room temperature and then separated by centrifugation from the mother liquid, washed several times with deionized water and dried at $100\text{ }^\circ\text{C}$ overnight. The solid was calcined at $400\text{ }^\circ\text{C}$ for 2 h in N_2 atmosphere (denoted as $\text{Cr}_2\text{O}_3\text{-N}$) and then reduced at $400\text{ }^\circ\text{C}$ in H_2 atmosphere for 2 h to obtain the final catalyst, which is denoted as Cr_2O_3 . The $\text{CrO}_3/\text{Cr}_2\text{O}_3$ catalyst was prepared by impregnating the Cr_2O_3 support with an aqueous solution of H_2CrO_4 (analytical grade, Sinopharm Chemical Reagent Co., Ltd., China) overnight. Then the suspension was evaporated at $80\text{ }^\circ\text{C}$ to obtain a solid, which was dried at $150\text{ }^\circ\text{C}$ for 4 h in N_2 atmosphere. The nominal content of CrO_3 in the catalyst was 10% (n/n), corresponding to $n_{\text{Cr(V)}}/n_{\text{Cr(III)}}=1:18$.

1.2 Catalyst characterizations

Surface areas of the catalysts were determined by the modified BET method from N_2 adsorption isotherms at liquid nitrogen temperature ($-195.7\text{ }^\circ\text{C}$) on a NOVA 4000e Surface Area & Pore Size Analyzer. Before the measurements, the samples were out-gassed at $300\text{ }^\circ\text{C}$ for 4 h under vacuum. X-ray diffraction (XRD) patterns of the catalysts were recorded on a PANalytical X'Pert PW3040/60 diffractometer with $\text{Cu K}\alpha$ radiation ($\lambda=0.154\text{ nm}$) operated at 40 kV and 40 mA. The patterns were collected in a 2θ range from 10° to 90° . Scanning electron micrographs (SEM) were recorded using Japan Hitachi S-4800 instrument with acceleration voltage 20 kV. Raman spectra were collected by a Renishaw RM1000 confocal microprobe under ambient conditions. The wavelength of the excitation laser was 514.5 nm. The scanning range was $200\sim 1\,800\text{ cm}^{-1}$. The reduction properties of the catalysts were measured by hydrogen temperature programmed reduction ($\text{H}_2\text{-TPR}$), which was carried out in a fixed-bed (i.d.=6 mm) reactor containing 20 mg of catalyst. The sample was heated in a flow of N_2 to $300\text{ }^\circ\text{C}$ at a rate of $10\text{ }^\circ\text{C}\cdot\text{min}^{-1}$, and kept at $300\text{ }^\circ\text{C}$ for 30 min. After cooling down to $100\text{ }^\circ\text{C}$, the sample was heated

from 100 to $500\text{ }^\circ\text{C}$ with a heating rate of $10\text{ }^\circ\text{C}\cdot\text{min}^{-1}$ under a mixture of 5% $\text{H}_2+95\%\text{ N}_2$ ($20\text{ mL}\cdot\text{min}^{-1}$). The amount of H_2 consumption was measured by a gas chromatograph with a thermal conductivity detector (TCD), which was calibrated by the quantitative reduction of a known amount of CuO powder. X-ray photoelectron spectra of the catalysts were obtained on an ESCALAB 250Xi instrument, with an $\text{Al K}\alpha$ X-ray source ($1\,486.6\text{ eV}$), under about $2\times 10^{-10}\text{ kPa}$ at room temperature and a pass energy of 20 eV . The binding energy (BE) of C1s core level at 284.6 eV was taken as the internal standard.

1.3 Catalytic testing

Before reaction, pre-fluorination was carried out in order to activate the catalyst. The pre-fluorination was performed in a stainless steel tubular reactor ($10\text{ mm (i.d.)}\times 300\text{ mm}$). 3 mL of the catalyst (about 4 g) was loaded in the reactor with a thermal couple placed in the middle of the catalyst bed to monitor the reaction temperature. The catalyst was heated at $300\text{ }^\circ\text{C}$ for 1 h in a N_2 flow ($40\text{ mL}\cdot\text{min}^{-1}$), followed by a mixture of 80% $\text{HF}+20\%\text{ N}_2$ (total flow rate of $50\text{ mL}\cdot\text{min}^{-1}$) at $400\text{ }^\circ\text{C}$ for 2 h. Then the catalyst was cooled down to the desired reaction temperature ($320\text{ }^\circ\text{C}$).

The fluorination reaction was carried out in the same reactor after the catalyst activation. The feed gas consisted a mixture of 2-chloro-1,1,1-trifluoroethane (HCFC-133a)+ $\text{HF}+\text{N}_2$ (3, 30, 10 $\text{mL}\cdot\text{min}^{-1}$, respectively), corresponding to a space velocity of 860 h^{-1} . The products were analyzed by a gas chromatograph (Shimadzu GC-2014) equipped with a flame ionization detector (FID) and a GS-GASPRO capillary column ($60\text{ m}\times 0.32\text{ mm}$) after the HF and HCl in the reaction effluent was neutralized by passing the effluent through an aqueous KOH solution.

2 Results and discussion

2.1 Catalytic behaviors for gas phase fluorination of HCFC-133a

Fig.1 shows the catalytic behaviors of the Cr_2O_3 and $\text{CrO}_3/\text{Cr}_2\text{O}_3$ catalysts for the fluorination of HCFC-133a at $320\text{ }^\circ\text{C}$. The Cr_2O_3 shows good stability during the reaction process, giving a steady state HCFC-133a

conversion of 18.5% and 2-chloro-1,1,1-trifluoroethane (HFC-134a) selectivity of 99.0%. As for the $\text{CrO}_3/\text{Cr}_2\text{O}_3$ catalyst, it gives high initial conversion (about 30.6%), at the expense of low selectivity to HFC-134a (73.0%). However, the catalyst deactivates rapidly, with the conversion declining to 20.0% after 9 h reaction and the selectivity gradually increasing to 99%. Fig.2 shows the area specific rates of Cr_2O_3 and $\text{CrO}_3/\text{Cr}_2\text{O}_3$ catalysts with time on stream. We observe that the Cr_2O_3 has steady reaction rate during the process while the area specific reaction rate of the $\text{CrO}_3/\text{Cr}_2\text{O}_3$ rapidly declines in the first 4 h reaction and it reaches the same level as that of the Cr_2O_3 catalyst. It shows that $\text{CrO}_3/\text{Cr}_2\text{O}_3$ catalyst has a very significant deactivation, while Cr_2O_3 catalyst is very stable.

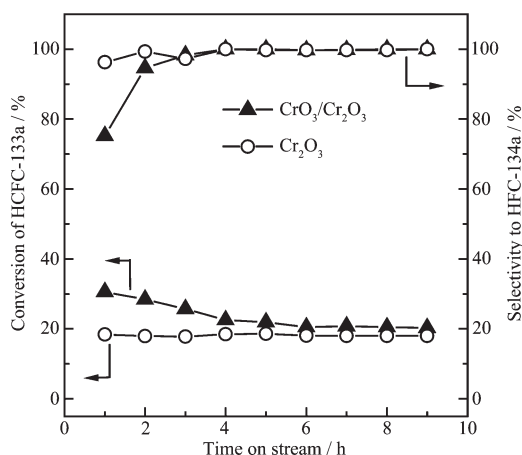


Fig.1 Catalytic performance of Cr_2O_3 and $\text{CrO}_3/\text{Cr}_2\text{O}_3$ catalysts for the fluorination of HCFC-133a at 320 °C

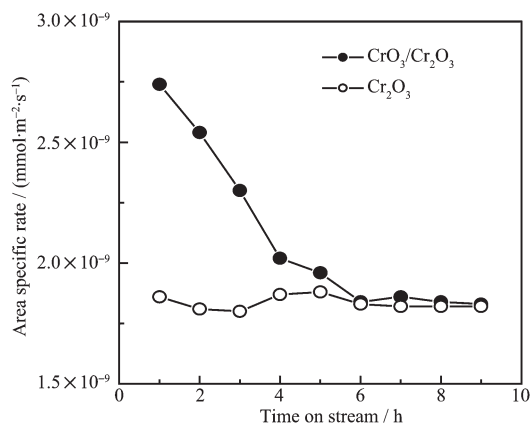


Fig.2 Area specific rates of Cr_2O_3 and $\text{CrO}_3/\text{Cr}_2\text{O}_3$ catalysts with time on stream

2.2 Characterizations of the catalysts

In order to investigate the properties of the catalysts, various characterizations were conducted. First of all, it is found that the $\text{CrO}_3/\text{Cr}_2\text{O}_3$ catalyst has slightly higher surface area ($62 \text{ m}^2\cdot\text{g}^{-1}$) than the Cr_2O_3 ($55 \text{ m}^2\cdot\text{g}^{-1}$) (Table 1) while the spent catalysts have similar surface areas compared to the fresh counterparts. Fig.3 shows the XRD patterns of the Cr_2O_3 and $\text{CrO}_3/\text{Cr}_2\text{O}_3$ catalysts before and after reaction. The diffraction peaks due to crystalline Cr_2O_3 (PDF 38-1479) are clearly observed both in the Cr_2O_3 and $\text{CrO}_3/\text{Cr}_2\text{O}_3$ catalysts. However, no diffraction peaks related to other Cr species are detected. Compared with the fresh catalysts, the spent ones show almost identical diffraction peaks, which implies that crystalline Cr_2O_3 is difficult to be fluorinated in HF atmosphere. In addition, the Cr_2O_3 catalyst has larger crystallite size than the $\text{CrO}_3/\text{Cr}_2\text{O}_3$ (Table 1). The corresponding spent catalyst has slightly larger crystallite size compared to the fresh one, indicating the growth of catalyst particles during the high temperature reaction. However, the essentially constant lattice parameters suggest that the hexagonal structure of the Cr_2O_3 remains intact during the reaction.

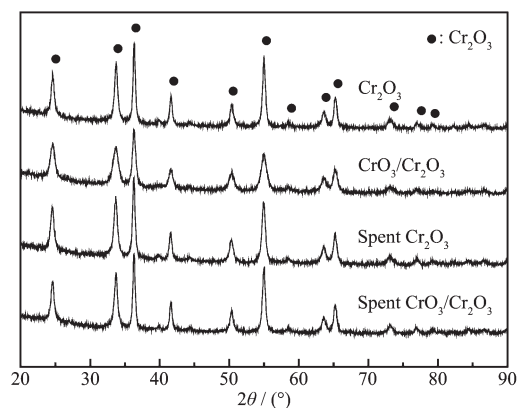
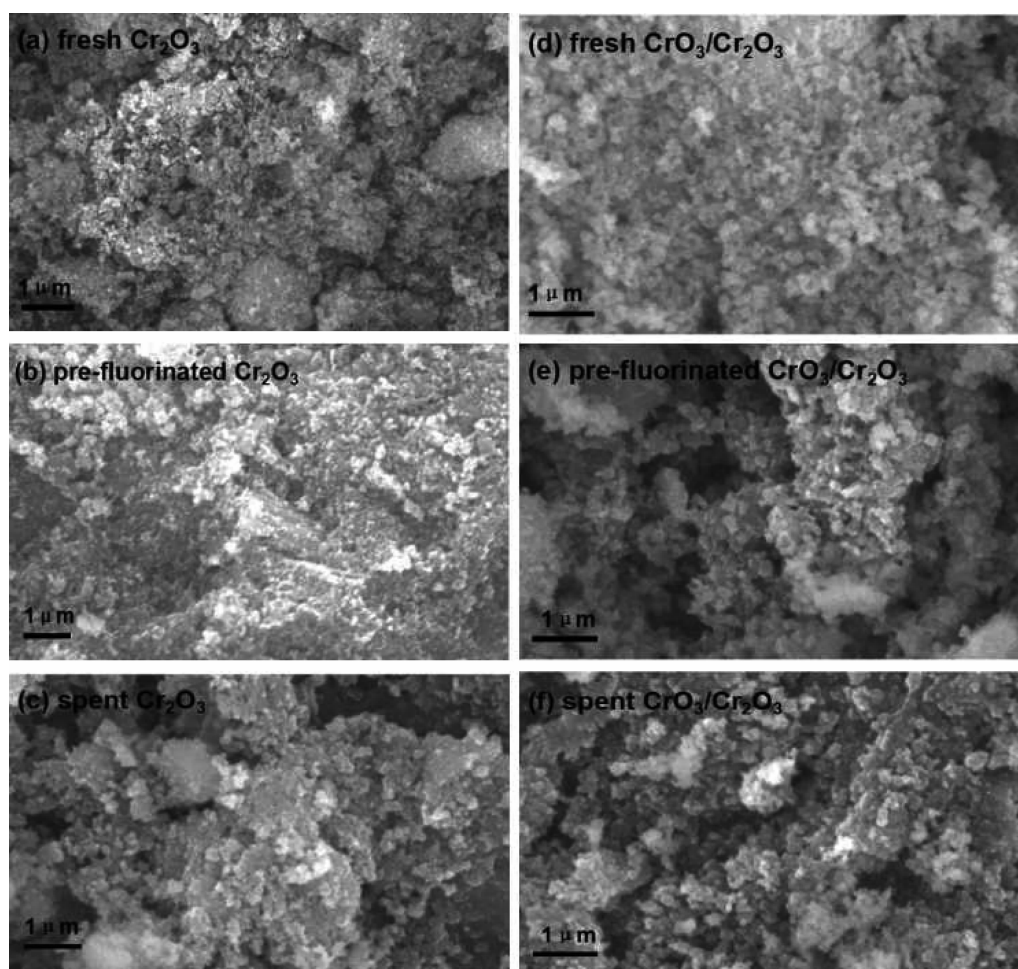


Fig.3 XRD patterns of the Cr_2O_3 and $\text{CrO}_3/\text{Cr}_2\text{O}_3$ catalysts before and after reaction

Fig.4 shows the SEM images of Cr_2O_3 and $\text{CrO}_3/\text{Cr}_2\text{O}_3$ catalysts under different conditions (fresh, pre-fluorinated and after reaction). The images of the fresh samples show nanoparticles of Cr_2O_3 and no porous structures are detected (Fig.4a and d). The pre-fluorinated and spent catalysts show no obvious

Table 1 Specific surface areas, crystallite sizes and lattice parameters of various catalysts

Catalyst	$S_{\text{BET}} / (\text{m}^2 \cdot \text{g}^{-1})$	Crystal size / nm	Lattice parameter / nm		
			<i>a</i>	<i>b</i>	<i>c</i>
Cr_2O_3	55	20.3	0.495 8	0.495 8	1.359 8
$\text{CrO}_3/\text{Cr}_2\text{O}_3$	62	15.5	0.495 7	0.495 7	1.359 1
Spent Cr_2O_3	54	24.2	0.496 0	0.496 0	1.359 0
Spent $\text{CrO}_3/\text{Cr}_2\text{O}_3$	60	17.0	0.495 8	0.495 8	1.360 0

**Fig.4** SEM images of fresh Cr_2O_3 , pre-fluorinated Cr_2O_3 and spent Cr_2O_3 (a~c), as well as fresh $\text{CrO}_3/\text{Cr}_2\text{O}_3$, pre-fluorinated $\text{CrO}_3/\text{Cr}_2\text{O}_3$ and spent $\text{CrO}_3/\text{Cr}_2\text{O}_3$ catalysts (d~f)

differences to the fresh ones, indicating that the pretreatment and reaction conditions exert no pronounced effect on the catalyst morphologies.

Fig.5 shows the H_2 -TPR profiles of the Cr_2O_3 and $\text{CrO}_3/\text{Cr}_2\text{O}_3$ catalysts. The Cr_2O_3 catalyst shows a very weak reduction peak in range of 350~600 °C, due to the reduction of trace high-valent Cr species in the catalyst^[29]. The presence of Cr(VI) species in the Cr_2O_3 catalyst are probably due to the formation of CrO_3 via the oxidation of Cr_2O_3 compound during the calcina-

tion process at 400 °C although it was then reduced. Similar findings of Cr(VI) were also reported in $\text{Y}_2\text{O}_3\text{-Cr}_2\text{O}_3$ catalyst systems^[30]. For the $\text{CrO}_3/\text{Cr}_2\text{O}_3$ catalyst, one intense but broad reduction peak is observed at 300 ~600 °C, which could be attributed to the reduction of high valent Cr species (e.g. Cr^{5+} , Cr^{6+})^[29]. Also, the calculated H_2 consumptions on the Cr_2O_3 and $\text{CrO}_3/\text{Cr}_2\text{O}_3$ catalysts are 0.02 and 0.61 $\text{mmol} \cdot \text{g}^{-1}$, respectively. According to the H_2 consumption values and assuming that all the high-valent Cr species are

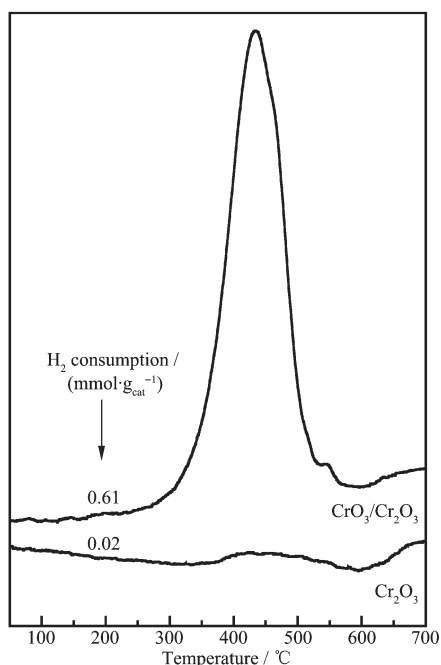


Fig.5 H_2 -TPR profiles of Cr_2O_3 and $\text{CrO}_3/\text{Cr}_2\text{O}_3$ catalysts

Cr(VI) , the contents of Cr(VI) species in these catalysts could be calculated, assuming the reduction during $300\sim 600\text{ }^\circ\text{C}$ is due to $2\text{CrO}_3 + 3\text{H}_2 \rightarrow \text{Cr}_2\text{O}_3 + 3\text{H}_2\text{O}$. The Cr(VI) contents in the Cr_2O_3 and $\text{CrO}_3/\text{Cr}_2\text{O}_3$ catalysts are 0.013 and $0.40\text{ mmol}\cdot\text{g}_{\text{cat}}^{-1}$, respectively. Note that for the $\text{CrO}_3/\text{Cr}_2\text{O}_3$ catalyst, the nominal Cr(VI) content is $0.68\text{ mmol}\cdot\text{g}_{\text{cat}}^{-1}$. Therefore, the lowered actual Cr(VI) content ($0.40\text{ mmol}\cdot\text{g}_{\text{cat}}^{-1}$) compared to the nominal value implies that part of the CrO_3 could transform to Cr_2O_3 during the thermal treatment ($150\text{ }^\circ\text{C}$ in N_2). These values suggest that in the Cr_2O_3 the Cr species dominantly exist in the form of Cr_2O_3 (Cr^{3+}), while the Cr species exist in forms of mixed high valent Cr^{6+} and Cr_2O_3 in the $\text{CrO}_3/\text{Cr}_2\text{O}_3$. Fig.6 shows the Raman spectra of the Cr_2O_3 and $\text{CrO}_3/\text{Cr}_2\text{O}_3$ catalysts before and after reaction. For all the catalysts, six Raman bands at $302, 342, 545, 610, 676$ and 1350 cm^{-1} are observed, which are attributed to Cr_2O_3 species^[31]. Compared to the Cr_2O_3 , the intensities of these bands are significantly lower in the $\text{CrO}_3/\text{Cr}_2\text{O}_3$ catalyst. In addition, a rather weak band at 1000 cm^{-1} assigned to Cr(VI) is also detected in all the catalysts^[32-34]. This presence of Cr(VI) species in these fresh catalysts is in consistent with the H_2 -TPR results (Fig.5). Moreover, calculation of I_{1000}/I_{545} ratio is used to quantitatively

compare the concentrations of Cr(VI) in the catalysts (Fig.6), where I_{1000} and I_{545} refer to the intensity of band at 1000 and 545 cm^{-1} , respectively. For the fresh catalysts, the I_{1000}/I_{545} ratio is 0.05 for the Cr_2O_3 catalyst, which is much lower than that for the $\text{CrO}_3/\text{Cr}_2\text{O}_3$ catalyst (0.28). This semi-quantitative comparison suggests that the Cr(VI) content is much higher in the $\text{CrO}_3/\text{Cr}_2\text{O}_3$ catalyst than that in the Cr_2O_3 catalyst, which is in good agreement with the H_2 -TPR results (Fig.5). For the spent $\text{CrO}_3/\text{Cr}_2\text{O}_3$ catalyst, the ratio is 0.12 . The lowered ratio compared with that for the fresh $\text{CrO}_3/\text{Cr}_2\text{O}_3$ catalyst (0.28) suggests either the loss of Cr(VI) species during the reaction process or the transformation of such species to low valent Cr species. Besides, the color of the $\text{CrO}_3/\text{Cr}_2\text{O}_3$ catalyst changed from black to green after 9 h reaction, which is the characteristic color of Cr(III) species. This observation again confirms the transformation of Cr species during the reaction process.

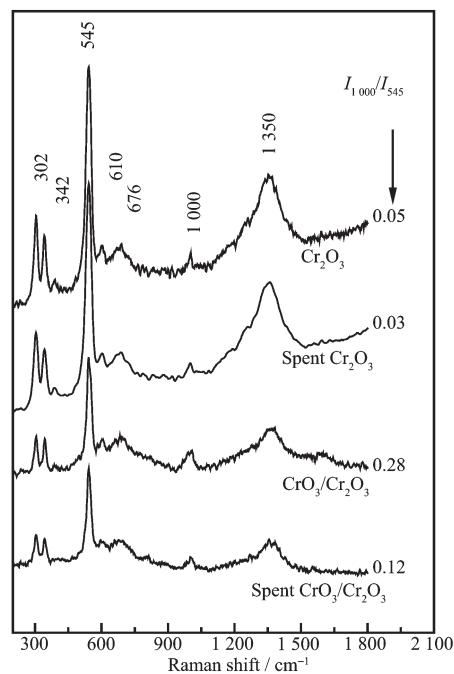


Fig.6 Raman spectra of Cr_2O_3 and $\text{CrO}_3/\text{Cr}_2\text{O}_3$ catalysts before and after reaction

XPS experiments were conducted to further investigate the surface structures of the Cr_2O_3 and $\text{CrO}_3/\text{Cr}_2\text{O}_3$ catalysts (Fig.7) and the detailed results are summarized in Table 2. For the N_2 thermal treated Cr_2O_3 catalyst ($\text{Cr}_2\text{O}_3\text{-N}$, Fig.7a), the $\text{Cr}2p_{3/2}$ peak was

deconvoluted into three peaks at binding energies of 578.1, 576.6 and 575.5 eV, assigned to CrO_3 , amorphous Cr_2O_3 and crystalline Cr_2O_3 ^[21], respectively. The Cr_2O_3 catalyst (reduced sample as used in reaction)

and the spent one (Fig.7b and c) show essentially the same features as the fresh one, suggesting the intact surface structure of this catalyst during the reaction which could explain the stability of the Cr_2O_3 . The

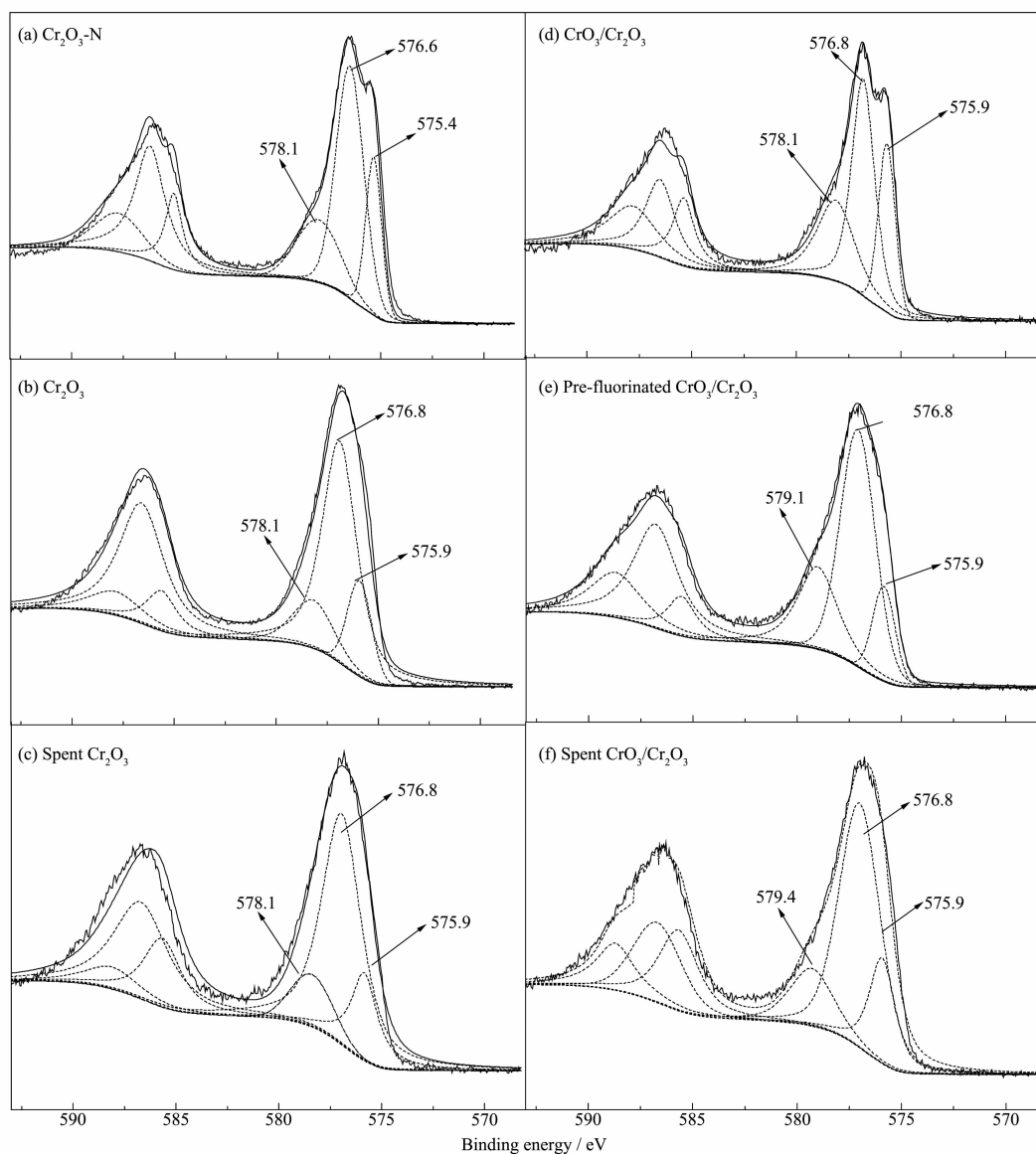


Fig.7 $\text{Cr}2p$ XPS spectra of $\text{Cr}_2\text{O}_3\text{-N}$, Cr_2O_3 and spent Cr_2O_3 (a~c), as well as as-prepared $\text{CrO}_3/\text{Cr}_2\text{O}_3$, pre-fluorinated $\text{CrO}_3/\text{Cr}_2\text{O}_3$ and spent $\text{CrO}_3/\text{Cr}_2\text{O}_3$ catalysts (d~f)

Table 2 Surface contents of different Cr species in various catalysts

Catalyst	Cr surface content / %				
	Crystalline Cr_2O_3	Amorphous Cr_2O_3	CrO_3	CrO_3F_y	CrF_3
$\text{Cr}_2\text{O}_3\text{-N}$	21.6	55.6	22.8	—	—
Cr_2O_3	15.8	68.3	15.8	—	—
Spent Cr_2O_3	19.8	67.7	12.5	—	—
$\text{CrO}_3/\text{Cr}_2\text{O}_3$	10.0	47.6	42.4	—	—
Pre-fluorinated $\text{CrO}_3/\text{Cr}_2\text{O}_3$	14.1	57.4	28.5 ($\text{CrO}_3 + \text{CrO}_3\text{F}_y + \text{CrF}_3$)		
Spent $\text{CrO}_3/\text{Cr}_2\text{O}_3$	19.7	63.1	—	—	17.2

presence of CrO_3 in the Cr_2O_3 at all stages (N_2 thermal treated, reduced and spent) is in good agreement with the Raman results (Fig.6). Moreover, the XPS analyses provide more reliable information on the Cr(VI) species compared to the Raman results (Fig.6). However, the concentrations of CrO_3 species differ in these three catalysts (Table 2). For example, the surface concentration of the Cr(VI) species in the N_2 thermal treated Cr_2O_3 ($\text{Cr}_2\text{O}_3\text{-N}$, 22.8%) is higher than those of the reduced Cr_2O_3 (15.8%), which implies the reduction of surface CrO_3 species. Also, compared to the reduced Cr_2O_3 , the spent Cr_2O_3 catalyst contains a lower content of surface Cr(VI) but a higher content of crystalline Cr_2O_3 , which indicates that some CrO_3 species transform to crystalline Cr_2O_3 during the high temperature reaction. Nevertheless, the finding of CrO_3 implies this species is quite stable in the catalyst, possibly due to the strong interaction between CrO_3 and Cr_2O_3 in this catalyst. For the fresh $\text{CrO}_3/\text{Cr}_2\text{O}_3$ catalyst (Fig.7d), it shows three deconvoluted peaks at binding energies of 578.1, 576.8 and 575.9 eV, assigned to CrO_3 , amorphous Cr_2O_3 and crystalline Cr_2O_3 , respectively^[23]. The spectrum of the fresh $\text{CrO}_3/\text{Cr}_2\text{O}_3$ contains the same features as the Cr_2O_3 catalyst (Fig.7b), except that the surface concentration of CrO_3 in the $\text{CrO}_3/\text{Cr}_2\text{O}_3$ is 42.4%. This much higher value compared to that in the Cr_2O_3 (15.8%) suggests that the $\text{CrO}_3/\text{Cr}_2\text{O}_3$ contains more CrO_3 species than the Cr_2O_3 , which again agrees with the Raman results (Fig.6). For the pre-fluorinated $\text{CrO}_3/\text{Cr}_2\text{O}_3$ catalyst (Fig.7e), the $\text{Cr}2p_{3/2}$ core level could be deconvoluted into three peaks at 579.1, 576.8 and 575.9 eV. The assignment of the peak at 579.1 eV is a little complicated and it might be due to a combination of CrO_xF_y species at 578.8 eV^[28,35] and CrF_3 species at 579.4 eV^[18]. The formation of such CrO_xF_y species may be due to the fluorination of CrO_x during the pretreatment with HF to form some CrO_xF_y species such as CrO_2F_2 , CrOF_4 , CrOF_3 , CrOF_2 and CrOF ^[36-37] and these species are regarded as the active species for F/Cl exchange reaction^[38-39]. Moreover, the formation of CrF_3 is probably due to the decomposition of such CrO_xF_y species as it was reported that CrOF_3 could decompose to

stable CrF_3 at 350 °C^[40]. After reaction, the spent $\text{CrO}_3/\text{Cr}_2\text{O}_3$ (Fig.7f) contains CrF_3 species with a BE of 579.4 eV, which could be due to the decomposition CrO_xF_y species during the reaction^[40]. In addition, since the surface CrF_3 content in the spent catalyst is less than 28.5% and the contents of crystalline and amorphous Cr_2O_3 in this sample increase compared to the pre-fluorinated one, it implies that some CrO_3 species could transform to Cr_2O_3 during the reaction, which is similar to the finding in the Cr_2O_3 catalyst (Fig.7c).

Based on the above results, two important issues could be clarified. The first issue concerns the contributions of different Cr species in the reaction. The high initial activity of the $\text{CrO}_3/\text{Cr}_2\text{O}_3$ catalyst (30.6%) indicates the important role of the high valent Cr(VI) species, which is in line with the comprehension that such species are crucial for the formation of catalytically active species such as CrO_xF_y ^[41]. However, the finding that the low valent Cr(III) compounds such as Cr_2O_3 is also active for the reaction suggests the role of low valent Cr species, which has been rarely recognized in literature^[28]. Since the Cr_2O_3 also contains a surface CrO_3 content of 15.8% (Table 2), an important question may arise that these CrO_3 species could also contribute in the reaction. To clarify this, an additional experiment was conducted.

Fig.8 compares the catalytic performance of the N_2 thermal treated Cr_2O_3 ($\text{Cr}_2\text{O}_3\text{-N}$) and reduced Cr_2O_3 catalyst (which was used in the reaction) and it is found that these two catalysts show almost identical performance. Considering the fact that the $\text{Cr}_2\text{O}_3\text{-N}$ contains a higher surface CrO_3 content than the reduced one (Table 2), it could be safely concluded that such CrO_3 species in the Cr_2O_3 hardly contribute in the reaction and the low-valent Cr(III) species in the Cr_2O_3 catalyst accounts for its reactivity. Besides, the stable performance of the Cr_2O_3 during the reaction provides some promising potentials in practical application. Moreover, it is interesting to quantify the contributions of Cr(III) and Cr(VI) species in the reaction. Considering that only the surface Cr species are involved in the reaction, the quantitative calculation of reactivity of the individual Cr species is

based on the following assumptions: (1) Assuming that a catalyst crystallite with a size of D (nm) consists of numerous close-packed Cr_2O_3 cells, then the number of Cr_2O_3 cell in the crystallite is $N_{\text{bulk}} = \pi D^3 / (6abc)$, where a , b , and c are lattice parameters of the Cr_2O_3 cell (average values of a , b and c are 0.496, 0.496 and 1.359 nm, respectively, Table 1). (2) The number of surface Cr_2O_3 cell in the crystallite is $N_{\text{surf}} = \pi D^2 / [(ab+ac+bc)/3]$. (3) Then, the proportion of the Cr_2O_3 cell on the surface is $N_{\text{surf}}/N_{\text{bulk}} = 3.75/D$. Since the Cr_2O_3 catalyst contains dominantly $\text{Cr}(\text{III})$ species, the initial reactivity of the $\text{Cr}(\text{III})$ could be calculated based on the results in Fig.1, which is $4.16 \times 10^{-5} \text{ mol}_{\text{HCFC-133a}} \cdot \text{mol}_{\text{Cr}(\text{III})}^{-1} \cdot \text{s}^{-1}$. For the $\text{CrO}_3/\text{Cr}_2\text{O}_3$ catalyst, it could be seen that the enhanced initial reactivity (reaction rate of the $\text{CrO}_3/\text{Cr}_2\text{O}_3$ -reaction rate of the Cr_2O_3 in 1st hour) compared to the Cr_2O_3 catalyst is due to the contribution of $\text{Cr}(\text{VI})$, and the content of $\text{Cr}(\text{VI})$ species in the $\text{CrO}_3/\text{Cr}_2\text{O}_3$ catalyst is $0.4 \text{ mmol} \cdot \text{g}_{\text{cat}}^{-1}$ (based on the result in Fig.5). Therefore, the initial

reactivity (reaction time of 1 h) of the $\text{Cr}(\text{VI})$ species is calculated to be $1.71 \times 10^{-4} \text{ mol}_{\text{HCFC-133a}} \cdot \text{mol}_{\text{Cr}(\text{VI})}^{-1} \cdot \text{s}^{-1}$. Such quantitative comparison clearly shows that the $\text{Cr}(\text{VI})$ species have much higher initial reactivity than the $\text{Cr}(\text{III})$ species (almost by 4-fold), which is in good agreement with the findings that high valent Cr species play important roles in the reaction^[18], due to the formation of some catalytically active species such as CrO_xF_y which was confirmed by the XPS results (Fig.7e).

The second issues concerns the catalyst stability and species transformation during the reaction. The deactivation of the $\text{CrO}_3/\text{Cr}_2\text{O}_3$ catalyst is attributed to two possible reasons. The first one is the loss of active species (*e.g.* CrO_xF_y) during the reaction through evaporation of volatile CrO_xF_y species. It was reported that compounds such as CrOF_4 have low boiling points which could be easily evaporated at $40 \sim 50^\circ\text{C}$ ^[40]. Indeed, the volatilization of such Cr species was confirmed in our experiment. Some precipitate with a color of pale green was observed in the condensed neutralizing solution, which was identified as $\text{Cr}(\text{OH})_3$. The generation of such $\text{Cr}(\text{OH})_3$ is most likely due to the reaction between gaseous Cr species with KOH when the exhaust gas passed through the neutralization solution. The second one is the transformation of CrO_xF_y species to stable but inactive CrF_3 compound, which is confirmed by XPS (Fig.7c) results. The inactiveness of CrF_3 compound is clarified by the fact that the $\text{CrO}_3/\text{Cr}_2\text{O}_3$ catalyst containing considerable surface CrF_3 content (Fig.7f) has the same performance as the Cr_2O_3 catalyst (Fig.1), which is similar to the findings by Chung et al.^[39]. Also, the coverage of such inactive

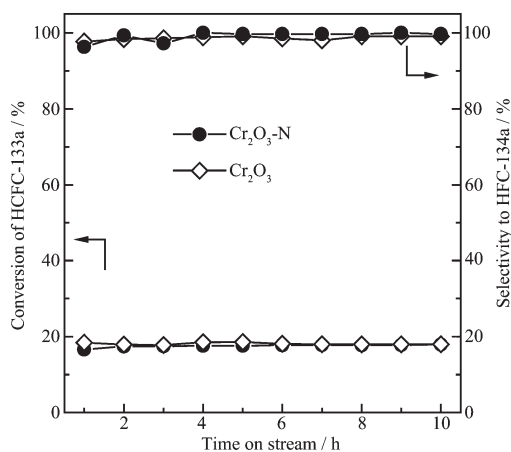


Fig.8 Comparison of catalytic performance of N_2 thermal treated Cr_2O_3 and Cr_2O_3 (reduced) catalysts

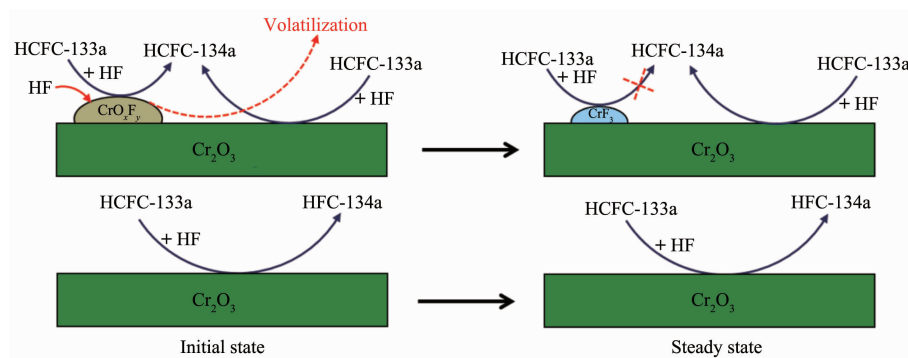


Fig.9 Possible reaction pathways over Cr_2O_3 and $\text{CrO}_3/\text{Cr}_2\text{O}_3$ catalysts at initial and steady states

CrF₃ on the Cr₂O₃ surface could account for the CrO₃/Cr₂O₃ catalyst deactivation (Fig.2).

Therefore, the possible reaction models on the Cr₂O₃ and CrO₃/Cr₂O₃ catalysts are illustrated in Fig.9. For the Cr₂O₃ catalyst (bottom panel), it is stable during the reaction, and HCFC-133a could react with HF on the surface to form HFC-134a. For the CrO₃/Cr₂O₃ catalyst (top panel), in addition to the reaction over the Cr₂O₃ support, the CrO_xF_y compounds generated during the pre-fluorination are very active for the reaction. However, these compounds could either volatilize or transform to stable but inactive CrF₃ during the reaction.

3 Conclusions

This work demonstrated that different species of chrome oxide catalyst have distinctively different behaviors in the vapor phase fluorination of HCFC-133a to synthesize HFC-134a. The Cr₂O₃ support containing dominantly Cr(III) species (amorphous or crystalline Cr₂O₃) is very stable during the reaction, although its reactivity is not high. On the contrary, the CrO₃/Cr₂O₃ catalyst containing high valent Cr species (Cr(VI)) could react with HF to form some catalytic active species such as CrO_xF_y. These species have high initial reactivity than the Cr₂O₃, but they volatilize during the reaction and could transform to stable but inactive CrF₃ species, which accounts for the catalyst deactivation.

References:

- [1] Cheng Y X, Fan J L, Xie Z Y, et al. *J. Fluorine Chem.*, **2013**, **156**:66-72
- [2] Cochon C, Corre T, Celerier S, et al. *Appl. Catal. A*, **2012**, **413** (3):149-156
- [3] Mao W, Wang B, Ma Y B, et al. *Catal. Commun.*, **2014**, **49** (2):73-77
- [4] Yoshimura T, Homoto Y, Yamada Y, et al. *US Patent*, 6011185. 1996-08-29.
- [5] Brunet S, Boussand B, Martin D. *J. Catal.*, **1997**, **171**(3):287-292
- [6] YU Hong-Bo(于洪波), WANG Yue-Juan(王月娟), PENG Xiao-Bo(彭小波), et al. *Chinese J. Inorg. Chem.*(无机化学学报), **2012**, **28**(5):905-909
- [7] Ünveren E, Kemnitz E, Lippitz A, et al. *J. Phys. Chem. B*, **2005**, **109**(9):903-1913
- [8] York S C, Cox D F. *J. Phys. Chem. B*, **2003**, **107**(13):5182-5189
- [9] ZHONG Yong-Hui(钟永辉), ZHOU Qi(周琪), LIU Jia-Qin(刘家琴), et al. *Chinese J. Inorg. Chem.*(无机化学学报), **2013**, **29**(10):2133-2139
- [10] Alonso C, Morato A, Medina F, et al. *Appl. Catal. B*, **2003**, **40**(3):259-269
- [11] Weckhuysen B M, Wachs I E, Schoonheydt R A. *Chem. Rev.*, **1996**, **96**:3327-3349
- [12] Rao J M, Sivaprasad A, Rao P S, et al. *J. Catal.*, **1999**, **184** (4):105-111
- [13] Lee H, Kim H S, Kim H, et al. *J. Mol. Catal. A: Chem.*, **1998**, **136**(3):85-89
- [14] Cho D H, Kim Y G, Chung M J, et al. *Appl. Catal. B*, **1998**, **18**(3):251-261
- [15] Teinz K, Manuel S R, Chen B B, et al. *Appl. Catal. B*, **2015**, **165**(5):200-208
- [16] Sekiya A, Quan H D, Tamura M, et al. *J. Fluorine Chem.*, **2001**, **112**:145-148
- [17] Quan H D, Tamura M, Matsukawa Y, et al. *J. Mol. Catal. A: Chem.*, **2004**, **219**(2):79-85
- [18] Kohne A, Kemnitz E. *J. Fluorine Chem.*, **1995**, **75**:103-110
- [19] Brunet S, Requieme B, Colnay E, et al. *Appl. Catal. B*, **1995**, **5**(4):305-317
- [20] He J, Lu J Q, Xie G Q. *Indian J. Chem. Technol.*, **2009**, **48A**: 489-497
- [21] Huang J J, Fu Y P, Wang J Y, et al. *Mater. Res. Bull.*, **2014**, **51**(2):63-68
- [22] Mierczynski P, Maniecki T P, Maniukiewicz W, et al. *React. Kinet. Catal. Lett.*, **2011**, **104**(2):139-148
- [23] He J, Xie G Q, Lu J Q, et al. *J. Catal.*, **2008**, **253**:1-10
- [24] Zhu Y, Fiedler K, Rüdiger St, et al. *J. Catal.*, **2003**, **219**:8-16
- [25] Adamczyk B, Boese O, Weiher N, et al. *J. Fluorine Chem.*, **2000**, **101**:239-246
- [26] Kemnitz E, Hess A, Rother G, et al. *J. Catal.*, **1996**, **159**(3): 332-339
- [27] Cuzzato P, Alberani P, Zappoli S, et al. *Appl. Catal. A*, **2007**, **326**(5):48-54
- [28] Xie Z Y, Fan J L, Cheng Y X, et al. *Ind. Eng. Chem. Res.*, **2013**, **52**(13):3295-3299
- [29] Xia Y S, Dai H, Jiang H Y, et al. *Environ. Sci. Technol.*, **2009**, **43**(11):8355-8360
- [30] Wang F, Fan J L, Zhao Y, et al. *J. Fluorine Chem.*, **2014**, **166** (2):78-83
- [31] Yim S D, Nam I S. *J. Catal.*, **2004**, **221**(7):601-611

- [32]Grosso E, Damin A, Bonino F, et al. *Chem. Mater.*, **2005**,**17**(9):2019-2027
- [33]Weckhuysen B M, Wachs I E. *J. Phys. Chem.*, **1996**,**100**:14437-14442
- [34]Kim D S, Tatibouet J M, Wachs E. *J. Catal.*, **1992**,**136**(3):209-221
- [35]Loustaunau A, Fayolle-Romelaer R, Celerier S, et al. *Catal. Lett.*, **2010**,**138**(3):215-223
- [36]Xing L Q, Lu J Q, Bi Q Y, et al. *J. Raman Spectrosc.*, **2011**,**42**:1095-1099
- [37]Hope E G, Jones P J, Levason W, et al. *J. Chem. Soc., Dalton Trans.*, **1985**:529-533
- [38]Kemnitz E, Hansen G, Kohne A. *J. Mol. Catal.*, **1992**,**77**(2):93-200
- [39]Chung Y S, Lee H, Jeong H D, et al. *J. Catal.*, **1998**,**175**(3):220-225
- [40]Hope E G, Jones P J, Tajik M, et al. *J. Chem. Soc., Dalton Trans.*, **1984**:2445-2447
- [41]Jia W Z, Jin L Y, Wang Y J, et al. *J. Ind. Eng. Chem.*, **2011**,**17**(6):615-620